Molecular dynamics and combined docking studies for the identification of Zaire Ebola Virus inhibitors

Kazeem O. Sulaiman[1,*], Temitope U. Kolapo[2,3], Abdulmujeeb T. Onawole[4], Md A. Islam[5,6], Rukayat O. Adegoke[7], Suaibu O. Badmus[7]

[1]Department of Chemistry, University of Saskatchewan, 110 Science Place, Saskatoon, Saskatchewan S7N 5C9, Canada.
[2]Department of Veterinary Parasitology and Entomology, University of Ilorin, P.M.B. 1515, Ilorin, Nigeria.
[3]Department of Veterinary Microbiology, University of Saskatchewan, 52 Campus Drive, Saskatoon, Saskatchewan S7N 5B4, Canada.
[4]Gas Processing Center, College of Engineering, Qatar University, P.O. Box 2713, Doha, Qatar
[5]Department of Chemical Pathology, Faculty of Health Sciences, University of Pretoria and National Health Laboratory Service Tshwane Academic Division, Pretoria, South Africa.
[6]School of Health Sciences, University of Kwazulu-Natal, Westville Campus, Durban, South Africa.
[7]Department of Pure and Applied Biology, Ladoke Akintola University of Technology, P.M.B. 4000, Ogbomoso, Nigeria.

[*]Correspondence to: *kosulaiman2008@yahoo.com*

Abstract

Ebola virus (EBOV) is a lethal human pathogen with a risk of global spread of its zoonotic infections, and *Ebolavirus Zaire* specifically has the highest fatality rate amongst other species. There is a need for continuous effort towards having therapies, as a single licensed treatment to neutralize the EBOV is yet to come into reality. This present study virtually screened the MCULE database containing almost 36 million compounds against the structure of a Zaire Ebola viral protein (VP) 35 and a consensus scoring of both MCULE and CLCDDW docking programs remarked five compounds as potential hits. These compounds, with binding energies ranging from -7.9 to -8.9 kcal/mol, were assessed for predictions of their physicochemical and bioactivity properties, as well as absorption, distribution, metabolism, excretion, and toxicity (ADMET) criteria. The results of the 50-ns molecular dynamics simulations showed the presence of dynamic stability between ligand and protein complexes, and the structures remained significantly unchanged at the ligand-binding site throughout the simulation period. Both docking analysis and molecular dynamics simulation studies suggested strong binding affinity towards the receptor cavity and these selected compounds as potential inhibitors against the Zaire Ebola VP 35. With respect to inhibition constant values, bioavailability radar and other physicochemical properties,

compound A (MCULE-1018045960-0-1) appeared to be the most promising hit compound. However, the ligand efficiency and ligand efficiency scale need improvement during optimization, and also validation via *in vitro* and *in vivo* studies are necessary to finally make a lead compound in treating Ebola virus diseases.

Keywords: Consensus scoring, Ebolavirus Zaire, Molecular docking, Molecular dynamics, Zoonotic infections.

List of Abbreviations:

ADMET: Absorption, distribution, metabolism, excretion and toxicity

BBB: Blood-brain barrier

CLCDDW: CLC drug discovery workbench

Compound A: MCULE-1018045960-0-1

EBOV: Ebola virus

EVD: Ebola virus diseases

HERG: Human ether-ago-go related gene

HIA: Human intestinal absorption

MD: Molecular dynamics

MM-GBSA: Molecular mechanics-generalized born surface area

PDB: Protein data bank

PGP: Permeability glycoprotein

SBVS: Structure-based virtual screening

VP: Viral protein

WHO: World health organization

1. Introduction

Ebola virus (EBOV) remains one of the most virulent pathogens known to man and it is the known causative agent for a severe illness called Ebola virus disease (EVD). The two concurrent outbreaks of EVD in Nzara of South Sudan and Yambuku of Democratic Republic of Congo (DRC) accounted for the first record of EVD in 1976 (Feldmann et al., 2011; Grard et al., 2011; WHO, 1978). However, its most famous outbreak in the history was lately witnessed

between 2014 and 2016 in West African countries, like Liberia, Guinea, and Sierra Leone (Bah et al., 2015; Choi et al., 2015; "WHO | WHO Director-General briefs media on outcome of Ebola Emergency Committee," 2016). In addition to the disturbing health effects in those countries, the Ebola epidemic also affected the socio-economic sectors of these countries significantly (The World Bank, 2015). The World Health Organization (WHO) declared the outbreak to be an international public health emergency in 2014 as it spread to other countries like Nigeria, Mali, Senegal, Spain, and the USA, but later withdrew the declaration on 29 March 2016, presumably due to the temporary success recorded in managing the menace of EVD. ("WHO | WHO Director-General briefs media on the outcome of Ebola Emergency Committee," 2016). Meanwhile, the recent resurgences of the epidemic in DRC, call for improved efforts towards curtailing its potential scourge as presently available vaccines are yet to be licensed.

Cuevavirus, Marburgvirus, and Ebolavirus are the three genera of the virus family called Filoviridae, and the genius *Ebolavirus* has five known species, namely *Bundibugyo, Reston, Sudan, Tai Forest* and *Zaire* (Bukreyev et al., 2014; Kuhn et al., 2010). The *Ebolavirus zaire* is the specie that was responsible for the famous 2014-2016 West African epidemics (Bah et al., 2015; Weyer, Grobbelaar, & Blumberg, 2015). Like other viruses in the Filoviridae family, EBOV replicates proficiently in many cells to activate the release of inflammatory chemical signals at high level and then causes a diseased state by overwhelming the soluble glycoprotein synthesis of infected cells as well as the host immune defenses (Onawole et al, 2018; Tosh, Sampathkumar, Feldmann, & al., 2014). Human beings only become infectious upon showing certain symptoms that are not so different from those for many other common diseases have some similar symptoms (Ye & Yang, 2015) and thus the possible delay in early notice of EBOV infections. The Zaire Ebola viral protein 35 (VP35) is crucial in the synthesis of viral mRNA, the replication of the negative-sense RNA viral genome, DNA silencing suppression, and viral pathogenesis (Brown et al., 2014; Haasnoot et al., 2007; Leung et al., 2010). Meanwhile, neutralizing antibodies play a significant role in the protection against EBOV infections. Thus, EBOV vaccine capable of inducing lasting neutralizing antibody response is highly desirable and VP35 is a worthy target candidate for consideration in the on-going research efforts towards identifying and developing the necessary and effective antiviral drugs against the EBOV.

Notably, discovering a new drug entails exorbitant and time-consuming processes but computational modeling offers a faster, cheaper, and dependable approach to the current drug

discovery processes and it minimizes animal sacrifice that occurs in the form of animal testing in the processes (Kapetanovic, 2008; Setlur, Naik, & Skariyachan, 2017). Moreover, virtual screening enables reduction of the computational sampling space and thus makes computational calculations more tractable (Barcellos et al., 2018; Cavuturu, Bhandare, Ramaswamy, & Arumugam, 2018; Islam & Pillay, 2018; Mirza & Ikram, 2016). Meanwhile, most recent reports on virtual screening experiments against the EBOV employ a small database of compounds and are based on homology models of the EBOV glycoprotein (Delgado-Soler, Ariñez-Soriano, Granadino-Roldán, & Rubio-Martinez, 2011; Villaseñor-Granados, García, Vazquez, & Robles, 2016). The correctness of homology technique depends on the model quality and so it is less satisfactory to use homology model, especially when the exact protein structure at high resolution is known. Nevertheless, homology modeling has proved to be a useful and reliable tool in several instances (Schwede, 2013). Having the crystal structures of the viral protein enables accurate finding of active sites and thus inhibitors designing.

Ren *et al.* (2016) recently reported new scaffolds with the aid of virtual screening against VP35 (Ren et al., 2016). However, a very small dataset of 144 compounds was screened while other ADMET properties of the selected hits were not as well predicted. Thus, a need for more exhaustive study towards identifying inhibitors against Zaire Ebola virus using consensus scoring and molecular dynamics simulation, formed the objectives of this study. The consensus scoring approach compares two or more methods of docking process, and thus significantly improves the virtual screening performance and advances the prediction of bound conformations and poses, besides giving a better prediction of potential leads (Feher, 2006). These competitive advantages of consensus scoring supported its choice in this study that involves screening of a significantly large database containing barely 36 million compounds against the crystal structure of the Zaire EBOV VP35. The physicochemical as well as ADMET properties of the selected potential hit compounds were predicted, alongside the molecular dynamic simulation studies. These hit compounds showed desiring efficacies against the EBOV pathogen and their optimized forms might as well secure necessary endorsement to be used for EVD treatment, upon assessing their performances in both *in vitro* and *in vivo* studies.

2. Methods and Materials

2.1. Target protein preparation and virtual screening

The target protein used was the Zaire Ebola viral protein 35 (VP35) which has been reported to be crucial in viral pathogenesis (Brown et al., 2014; Haasnoot et al., 2007; Leung et al., 2010). The target protein (PDB ID: 4IBB), that was downloaded from the protein databank, has a resolution of 1.752 Å and this suggests its good quality as a resolution of 2.0 Å is the recommended maximum for a good structural protein (Hajduk, Huth, & Tse, 2005). The drug discovery studio visualizer (BIOVIA, 2015) was used to determine the binding pocket. The protein structure PDB ID: 4IBB exists as a dimer and in a complexed form such that using the protein for molecular docking without removing the initial ligand would lead to clashes in interactions of the ligand present in the protein and the ligands from the virtual screening (C A Lipinski, Lombardo, Dominy, & Feeney, 2001; Christopher A. Lipinski, 2004). The goal is to bind the ligands from the virtual screening to the active site of the complexed protein. The PDB site record option tool in the drug discovery studio (BIOVIA, 2015) was used to define the binding site area (Fig. 1). The initial complexed ligand was used as reference to define the binding pocket giving the parameters as -1.724, 19.971 and 22.566 for the X, Y and Z axes with a radius of 8.9 Å. This binding pocket has been confirmed experimentally using NMR and was reported to include residues such as ALA 221, ARG 225, ASP 302, GLN 241, LEU 242, LYS 248, LYS 251, ILE 295, ILE 297, PHE 328 and PRO 293 (Brown et al., 2014). Chain B was selected (actually either A or B can be selected as it is a dimer) while Chain A and all other molecules in the complex structure including water and the complexed ligands were removed to avoid their possible interactions during the virtual screening process. The ligands used for the virtual screening were gotten from the Mcule database (Kiss, Sandor, & Szalai, 2012) which contained exactly 35,742,734 compounds as at that the time of this work. The virtual screening was done using AutoDock Vina (Trott & Olson, 2010) with the aid of cloud computing which alleviated the computational cost. The workflow parameters for filtering the compounds in the Mcule database for virtual screening were the same as previously reported (Onawole et al, 2017). This enabled the screened compounds to have drug likeness attributes based on their physicochemical properties.

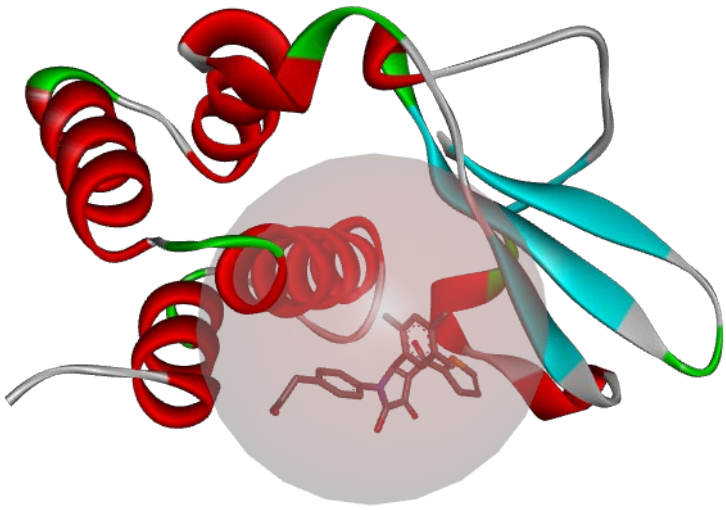

Fig. 1: The binding pocket of the initial complex ligand from PDB highlighted in red (chain B) used for virtual screening.

2.2. Consensus scoring

The flowchart (Fig. 2) depicts the steps involved in the entire selection process. The top scored 500 compounds were selected based on the docking scores in the first virtual screening using Auto Dock VINA. The drug like properties used to filter the 100, 000 compounds, sampled randomly from the Mcule database of about 36 million compounds are: the filtered compounds should not have more than 10 rotatable bonds; a maximum of 5 halogen atoms and 5 chiral centers; a minimum of 10 heavy atoms and a minimum of 1 aromatic ring; and finally should not violate more than one of the Lipinski's rule of five (RO5) (C A Lipinski et al., 2001; Christopher A. Lipinski, 2004) These compounds (Table S1) were then used as the input ligands for the second structure-based virtual screening (SBVS) using CLC drug discovery workbench (CLCDDW) (Knudsen, Bjarne Knudsen, 2016). The two docking protocols used have been assessed to give a low number of false positives (Pecina et al., 2017; Xu, Lucke, & Fairlie, 2015), and thus make excellent choices for consensus scoring. Moreover, AutoDock Vina which was the main docking protocol used in predicting binding energy was recently adjudged one of the best docking programs in estimating the free energy of binding in a recent study (Z. Wang et al., 2016). The same binding pocket parameter used for the initial SBVS was also implemented for the second SBVS to maintain consistency. All other parameters were set to default. The rank voting method (Feher, 2006) was

used to determine the selected compounds by normalizing and comparing the top scored 5% compounds from both virtual screenings (Figs S1 and S2).

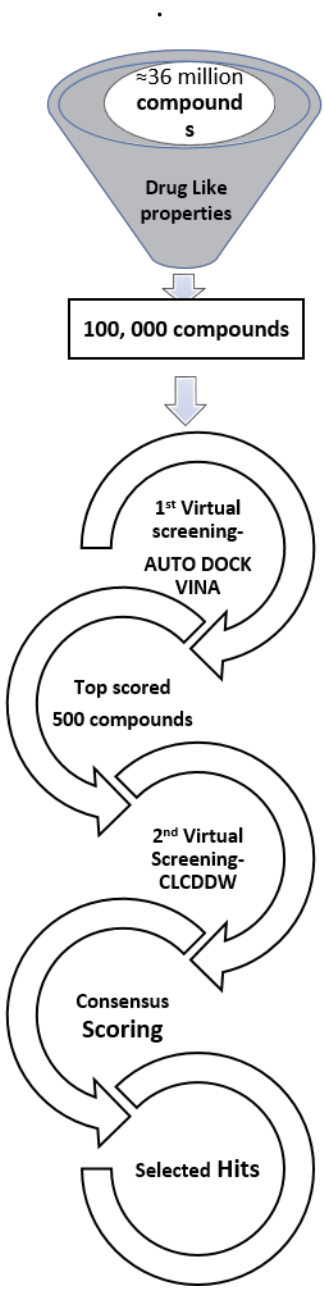

Fig. 2: Flowchart showing the methodology.

2.3 Molecular Dynamics

Molecular dynamics (MD) simulation was performed on the docked poses between Ebola virus protein and the selected screened compounds from Auto Dock Vina, using the Amber14 tool

(Salomon-Ferrer, Case, & Walker, 2013), installed on the CHPC server (https://www.chpc.ac.za/index.php/resources/lengau-cluster). The ff99SB force field35 was implemented with the explicit TIP3P water model box (Lindorff-Larsen et al., 2010), with a minimum distance of 8 Å. Ligands were parameterized using the general amber force field (GAFF) (J. Wang, Wang, Kollman, & Case, 2006; J. Wang, Wolf, Caldwell, Kollman, & Case, 2004) with Antechamber while missing hydrogen atoms were added using the Propka3.1 (Olsson, Søndergaard, Rostkowski, & Jensen, 2011), followed by sodium ions neutralization of the system with the aid of the Leap program of Amber14. At first, systems were partially minimized with 500 kcal/mol restrained force on the solute molecule, using 750 cycles of the steepest descent, followed by 2500 cycles of the conjugate gradient method. After that, systems were full minimized by conjugate gradient method for 1500 cycles, followed by heating gradually from 0 to 300 K with 10 kcal/mol harmonic restraint to ensure the solute was fixed. Langevin dynamics method was used to control the temperature using a collision frequency of 1.0 ps^{-1}. The systems were equilibrated for two ns at 300 K while keeping 1 bar of pressure constant. Using the SHAKE algorithm (Andersen, 1983), bonds were constrained involving hydrogen atoms. The MD was run for 50 ns with a time step of 2 fs and the MD trajectories were analysed for root mean square deviation (RMSD), root mean square fluctuation (RMSF) and Radius of gyration (Rg) for which the ptraj and cpptraj (Roe & Cheatham, 2013) module of Amber14 was used.

2.4 Free energy calculations using MM-GBSA approach

Molecular Mechanics-Generalized Born Surface Area (MM-GBSA) method (Genheden & Ryde, 2015) was used to quantitatively measure the binding strength between the receptor and ligands. The distribution of binding free energy can be expressed as given below:

$$\Delta G_{(bind,aq)} = \Delta G_{(bind,vacuum)} + \Delta G_{(bind,complex)} - \Delta G_{(bind,ligand)} \Delta G_{(bind,receptor)} \ldots (1)$$

The electrostatic component of the solvation free energy in the MM-GB method can be calculated by solving Generalized Born (GB) equation (2) and an empirical term for hydrophobic contribution is added.

$$\Delta G_{aq} = \Delta G_{GB} + \Delta G_{hydrophobic} \ldots\ldots\ldots\ldots\ldots\ldots\ldots\ldots (2)$$

The average interactions energies of proposed screened molecules and receptor were calculated from 50000 snapshots extracted from 50 ns of MD trajectories.

3. Results and discussion

3.1. Docking Analysis

The structure PDB ID: 4IBB consisting of two chains with a total of 243 residues was further validated for protein quality using Ramachandran plot (Ramachandran & Sasisekharan, 1968) which shows the allowed values of ψ (Psi) against φ (Phi) angles for a particular amino acid (Fig. 3). A perfect score of 0% outlier was obtained while the favored and allowed region have a combined total of more than 90 % to indicate the exceptional quality and thus reliability for molecular docking (Hooft, Sander, & Vriend, 1997; Kleywegt & Jones, 1996; Lovell et al., 2003). The top and bottom left regions of the Ramachandran plot correspond to the β-pleated and right handed α-helices while the middle of the right region signifies the left-handed α-helices.

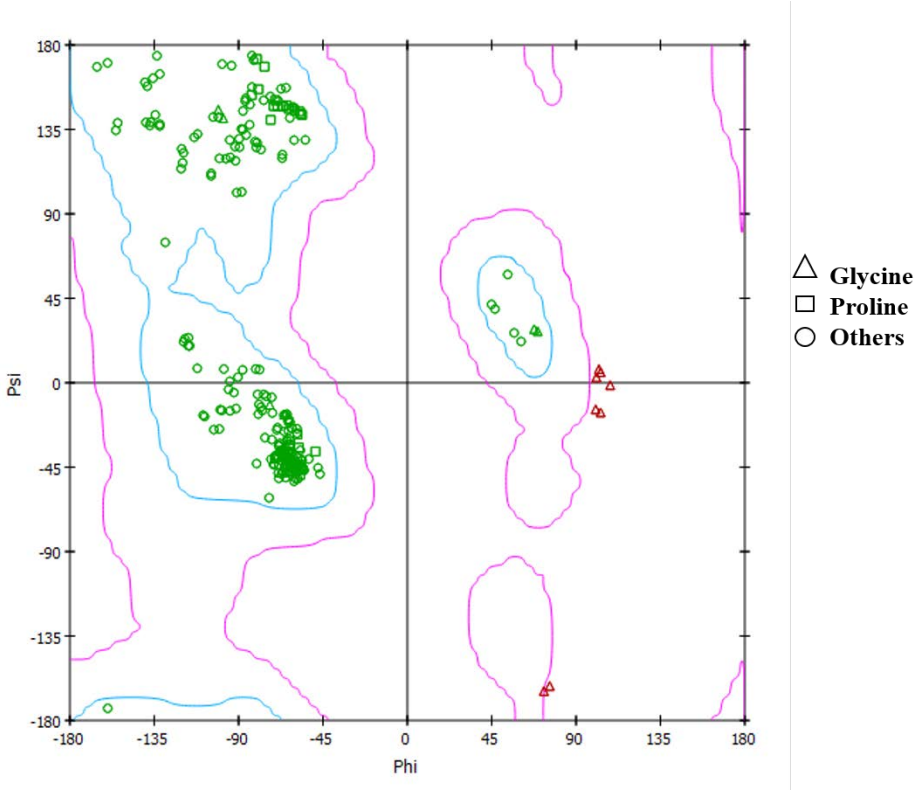

Fig. 3: Ramachandran plot of PDB:4IBB.

The results from both virtual screenings were normalized such that numbers close to 1 and 0 correlate with the top and bottom scored compounds respectively. A rank voting method

(Cerqueira et al., 2015) that compares the top 5% compounds of the normalized scores in each virtual screening was then used for consensus scoring. This gave rise to five selected compounds: MCULE-1018045960-0-1(2-[(7R)-7-(4-chlorophenyl)-5-phenyl-7H-tetrazolo[1,5-a]pyrimidin-4-yl]-N-[(4-fluorophenyl)methyl]acetamide), MCULE-2819757532-0-4 ((1S,5R,9S)-7-benzyl-3-methyl-1,5-dinitro-9-phenacyl-7-azabicyclo[3.3.1]non-2-en-4-one) , MCULE-4741178768-0-1(10-[4-(dimethylamino)anilino]-12-(4-methyl-1-piperidyl)-15-oxa-14-zatetracyclo[7.6.1.0^{2,7}.0^{13,16}]hexadeca-1(16),2,4,6,9,11,13-heptaene-8-one), MCULE-8041377389-0-1(N-[3-chloro-4-(3-oxopiperazin-1-yl)phenyl]-2-[5-(2-fluorophenyl)oxazol-2-yl]benzamide) and MCULE-8443281251-0-1 (3-(3-dibenzothiophen-4-ylphenyl)-N-[(2,6-difluorophenyl)methyl]imidazole-4-carboxamide), that are subsequently referred to as hit compounds A, B, C, D and E respectively (Fig. 4). The ranking positions for all the virtually screened compounds are presented elsewhere (Figs S1 and S2) but those for selected five compounds are presented in Fig. 5. Compound A was the fifth and the seventeenth ranked ligand while compound B was the twenty-second and sixth ranked ligand in Auto Dock Vina and CLCDDW docking respectively. Compound C was the seventeenth and tenth ranked ligand, compound D was the twelfth and twenty-fifth ranked ligand and compound E was the first and third ranked ligand in Auto Dock Vina and CLCDDW docking respectively.

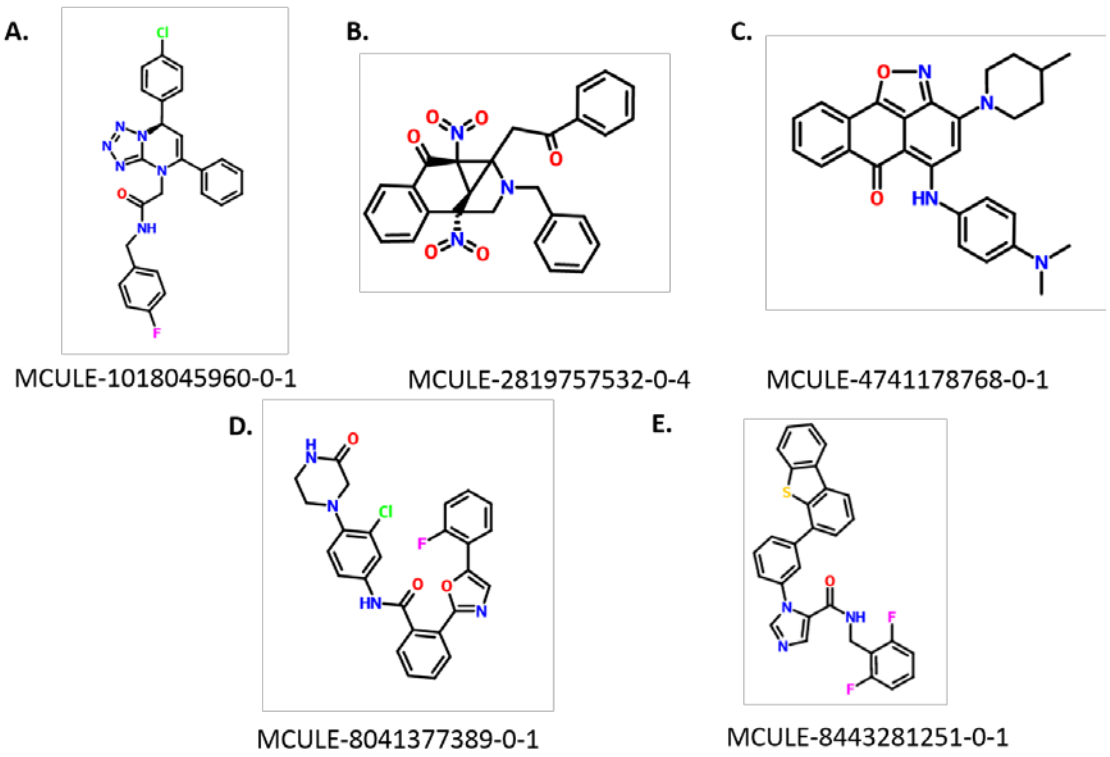

Fig. 4: The structures of the selected hit compounds.

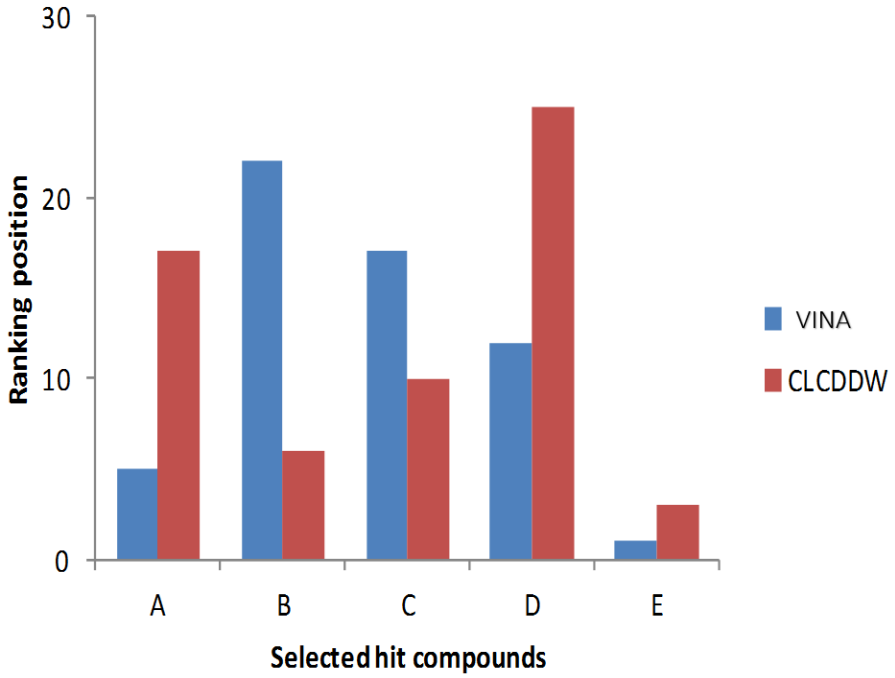

Fig. 5: The ranking positions of the selected hit compounds.

3.2. Physicochemical assessments of the selected hit compounds

The Lipinski's rule of five (RO5): molecular mass < 500; Hydrogen-bond donors (HBD) < 5; Hydrogen-bond acceptors (HBA) < 10; and LogP < 5 (Christopher A. Lipinski, 2000, 2004); allows prediction of physicochemical properties and hence the drug likeness of a compound. While all other physicochemical properties were calculated using Mcule's property calculator, WLogP that was estimated using the developed method by Wildman and Crippen (Wildman & Crippen, 1999). The selected five compounds, from the consensus scoring method, obey the RO5 except for compounds C and D that have WlogP values of 5.7 and 7.8 (Table 1). Also, these compounds have less than ten rotatable bonds (RTB) and 100 Å polar surface area (PSA), except compound B that has a PSA of 129.02 Å. These obtained values suggest that these compounds are orally bioavailable (Camp, Garavelas, & Campitelli, 2015). Besides, we employed Swiss ADME tool that affords the bioavailability radar (Fig. 6), which gives a quick glimpse of the drug likeness of a compound (Daina, Michielin, & Zoete, 2017). In Fig. 6, the pink area denotes the optimal area for each property and INSATU (Unsaturation) is expected to be in the range of 0.25 and 1 while INSOLU (Insolubility) is in the range of 0 and 6. LIPO, FLEX, SIZE and POLAR all refer to logP, rotatable bonds, molecular weight and polar surface area respectively. Compound B was the best of the selected compounds as it falls within the optimal range for all parameters. A trend of B > A > D > C > E can be obtained from both the Lipinski's RO5 and bioavailability radar.

Table 1: Physicochemical properties of the selected compounds.

NAME	A	B	C	D	E
Formula	$C_{25}H_{20}ClFN_6O$	$C_{27}H_{23}N_3O_6$	$C_{28}H_{28}N_4O_2$	$C_{26}H_{20}ClFN_4O_3$	$C_{29}H_{19}F_2N_3OS$
Mass (g/mol)	474.92	485.49	452.55	490.91	495.54
WlogP	4.12	4.18	5.7	4.46	7.8
HBA	5	7	3	5	4
HBD	1	0	1	2	1
Rotatable bonds	7	7	4	6	6
Polar Surface Area (PSA)/$Å^2$	75.94	129.02	61.61	87.47	75.16
RO5 violations	0	0	0	0	1
Heavy atoms (HA)	36	36	34	35	36
Log S (Solubility)	-6	-5.16	-6.93	-5.79	-7.52
Solubility class	Moderate	Moderate	Poor	Moderate	Poor

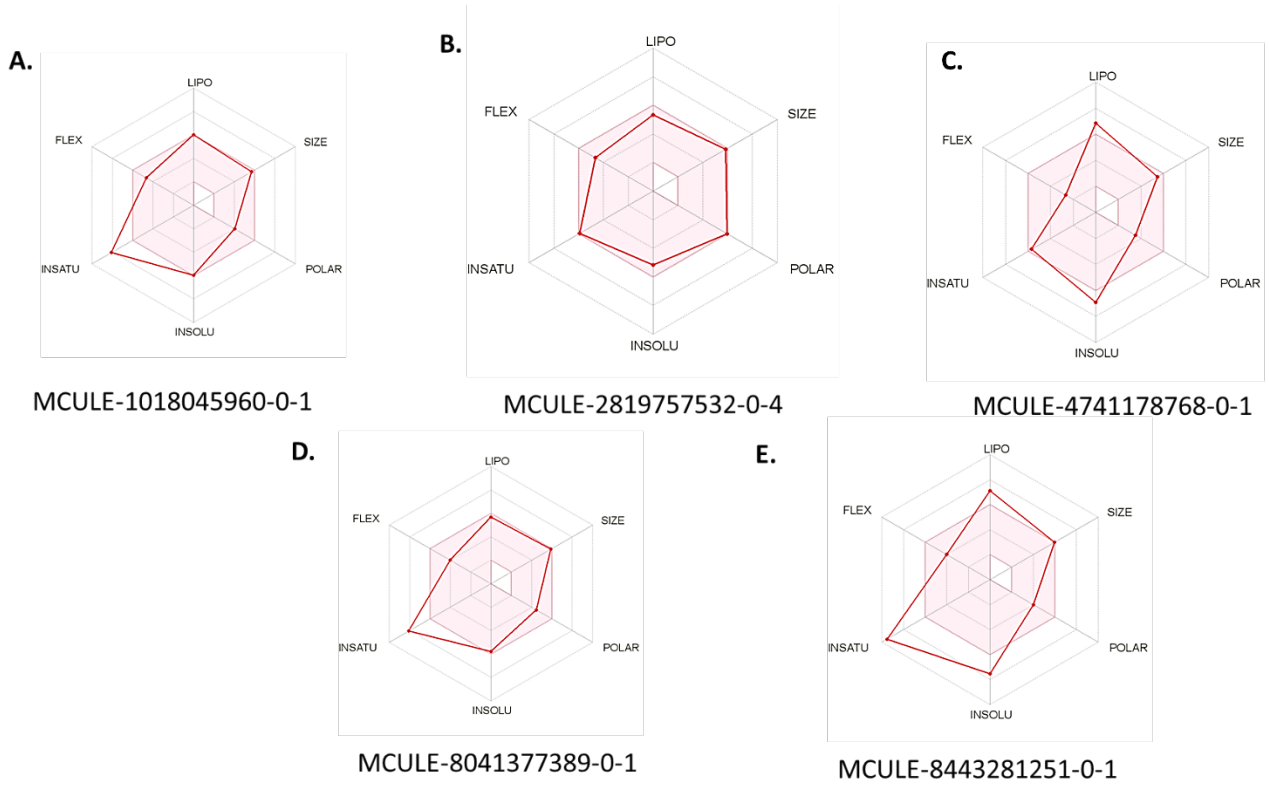

Fig. 6: The bioavailability radar for the selected hit compounds

The predicted bioactivity of the selected compounds, as well as their respective AutoDock Vina and CLCDDW docking scores are presented in Table 2. Specifically, the AutoDock Vina docking score corresponds to the predicted binding energy (B.E.) (Trott & Olson, 2010). The calculated inhibition constant (Ki) was obtained using equation (3) (Jedrzejas, Singh, Brouillette, Air, & Luo, 1995) where R is the gas constant (1.987×10^{-3} kcal/K-mol)) and T (298.15 K) is the absolute temperature of the protein-ligand complex. All the selected five compounds qualify as either hit or lead compounds considering their low Ki values in the micromolar range (0.3 – 1.6 µM) to imply high potency (Hughes, Rees, Kalindjian, & Philpott, 2011; Polanski, Tkocz, & Kucia, 2017; Reynolds & Reynolds, 2017). Specifically, only compounds A and E are predicted to be the most potent with Ki values of 0.7 and 0.1 µM respectively. Nevertheless, further optimization is required to lower their Ki values to 10 nM or less to qualify them as drug molecules. All other ligand efficiency related parameters were derived from the binding energy and thus calculated using equations (4-6). The Fit Quality (FQ) and Ligand Efficiency Lipophilic Price

(LELP) values for these compounds agree with the thresholds for these parameters and FQ value of 0.8 qualifies a compound as a hit (Hopkins, Groom, & Alex, 2004).

$$ki = e^{(-\Delta G/RT)} \quad (3)$$

$$\text{Ligand Efficiency } (LE) = -\text{B. E.} \div \text{H. A.} \quad (4)$$

$$\text{LE}_{\text{scale}} = 0.873e^{-0.026\times \text{H.A.}} - 0.064 \quad (5)$$

$$LELP = LogP \div \text{LE} \quad (6)$$

$$FQ = LE \div \text{LE}_{\text{scale}} \quad (7)$$

Table 2: Bioactivity prediction of the selected compounds

BIOACTIVITY	A	B	C	D	E
CLCDDW docking score	-60.1	-62.4	-61.6	-59.3	-64.6
AutoDock Vina docking score / (kcal/mol)	-8.4	-7.9	-8.0	-8.1	-8.9
Ki (μM)	0.7	1.6	1.4	1.2	0.3
Ligand Efficiency (LE) /(kcal/mol/heavy atom)	0.2	0.2	0.2	0.2	0.2
LE_Scale	0.3	0.3	0.3	0.3	0.3
Fit Quality (FQ)	0.8	0.8	0.8	0.8	0.9
Ligand-efficiency-dependent lipophilicity (LELP)	-8.4	-7.9	-8.0	-8.1	-8.9

Ki value should be in the micromolar range for a compound to be a hit; FQ recommended to be ≥ 0.8; full range of optimal LELP values is −10 to +10.

3.3. ADMET properties prediction

The boiled egg diagram illustrates the human intestinal absorption (HIA) and the brain penetration (Fig. 7). The white region (albumin) and the yellow region (yolk) correspond to the area where there is a high chance of HIA and brain penetration respectively. Only compound A falls within the yolk region to imply its high chance of being absorbed by the gastrointestinal tract and penetration into the brain. Furthermore, the molecular framework of Compound A consists of

fragment -N-C-C= that is predictive of having positive effect for increase in HIA (Radchenko, Dyabina, Palyulin, & Zefirov, 2016; Wessel, Jurs, Tolan, & Muskal, 1998) and the predicted good blood brain barrier (BBB) permeation is due to the presence of double and stereochemical 3D bond, alongside the following element: N, O, F, and Cl (Toropov, Toropova, Beeg, Gobbi, & Salmona, 2017). Hence, compound A has some molecular features that enable the prediction of its high chance of penetrating gastrointestinal tract and blood brain barrier. In contrast, compounds C and D fall within the white region to signify their high chances of being absorbed by the gastrointestinal tract only, while compounds B and E fall into the outlier category as they are outside the BOILED-Egg region. Also, the blue and red colored circles correspond to substrates (PGP+) and non-substrates (PGP-) of the permeability glycoprotein (PGP). The PGP reduces the efficacy of PGP+ compounds since it pumps them back into the intestinal lumen in the liver. Compounds A, B and E are PGP-, hence they are non-substrates while compounds B and C are PGP+, and hence they are substrates. Concerning the solubility, compounds A, B, and D amongst the selected compounds are moderately soluble while compounds C and E are poorly soluble compounds for having log S values outside the range of -1 to -6 (Tsaioun & Kates, 2011).

The toxicity properties were predicted using the pkCSM web tool (Pires, Blundell, & Ascher, 2015) and the obtained results are presented in Table 3. The AMES toxicity determines the mutagenicity of a compound and compounds A, E and C can be predicted to be non-mutagenic. The HERG (Human ether-ago-go gene) inhibition is related to ventricular arrhythmia which can be fatal (Sanguinetti & Tristani-firouzi, 2006). Hence, it is best that potential drug candidates are not HERG inhibitors. Fortunately, all the selected compounds are non-inhibitors of HERG. As the Ebola virus disease also affects the skin, the selected hit compounds were tested for their skin sensation and all of them are predicted to be safe for dermal application.

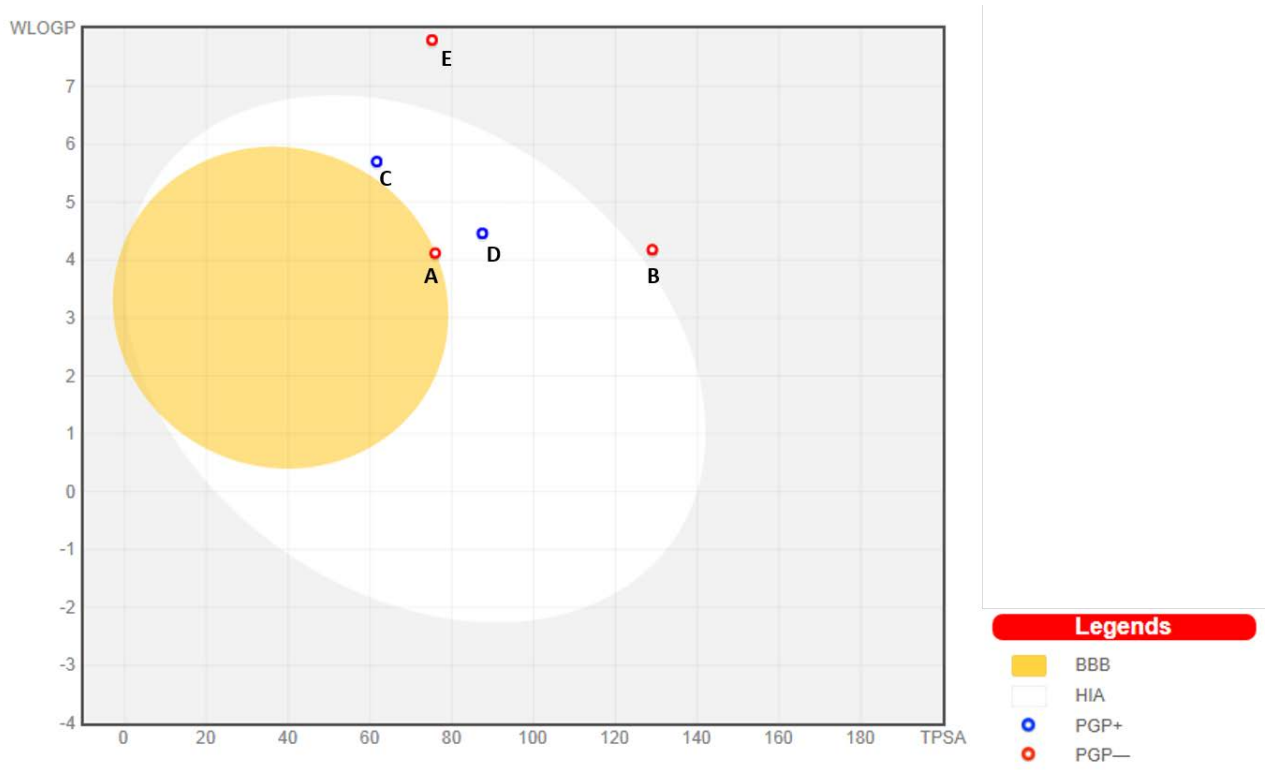

NB: The white region is the physicochemical space of molecules with highest probability of being absorbed by the gastrointestinal tract, and the yellow region (egg yolk) is the physicochemical space of molecules with highest probability to permeate to the brain. The egg yolk and white areas are not mutually exclusive.

Fig. 7: The EGG-BOILED model of the selected compounds.

Table 3: The toxicity properties of the selected hit compounds

Model Name	**A**	**B**	**C**	**D**	**E**	**Unit**
AMES toxicity	No	Yes	No	Yes	No	Categorical (Yes/No)
hERG inhibitor	No	No	No	No	No	Categorical (Yes/No)
Skin Sensitisation	No	No	No	No	No	Categorical (Yes/No)

3.4. Binding modes and molecular interactions

The molecular interactions and binding modes give insight into the mode of action of the selected compounds when bound to the target protein. The mode of action is very important in the optimization stage since a compound may be modified to increase its binding affinity, by

interacting with more amino acids that present in the target protein. The binding modes and molecular interactions of the selected compounds show that they have similar binding pockets. Albeit only the binding modes (Fig. 8) and molecular interactions (Fig. 9) of compound A in both Auto Dock Vina and CLCDDW are discussed due to its most promising properties concerning its bioavailability radar, K_i value and other physicochemical properties among the selected five compounds, similar results for other compounds B to E are presented in Figs. S3-S10. Compound A interacts with the same set of amino acids to indicate the same binding pocket in both Auto Dock Vina and CLCDDW docking as both programs have different scoring algorithms and hence different poses are generated for the same compound in the active site. Hence, the difference in their molecular interactions and docking score for the same compound. Nevertheless, the consensus scoring approach aims to reduce the rate of false positives hence leading to higher hit rates. Moreover, there is a need to further validate the results using experimental methods such as *in vitro* and *in vivo* to know for certain the actual binding pose and affinity of the selected hits.

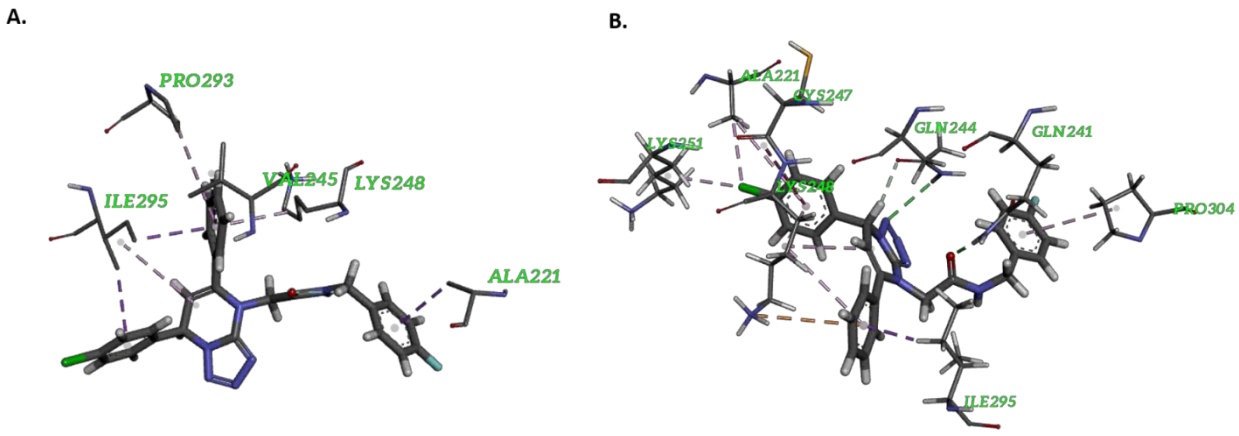

Fig. 8: The binding modes of compound A in (a) Auto Dock VINA and (b) CLCDDW.

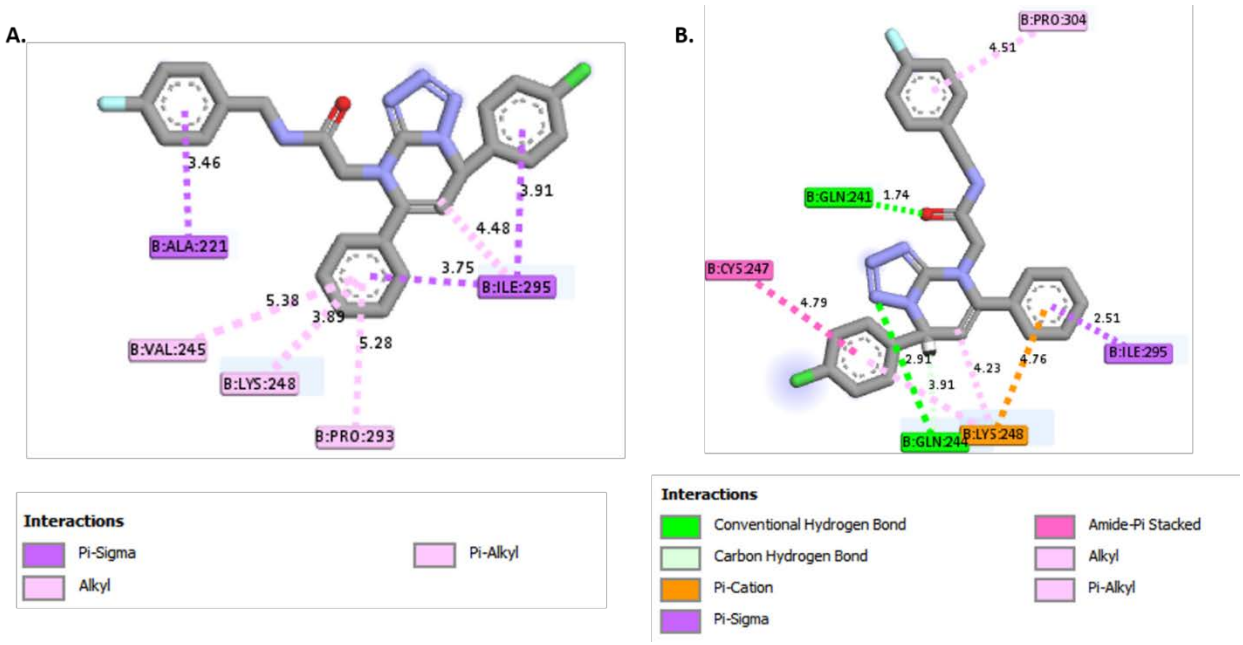

Bond lengths are in Angstroms

Fig. 9: The molecular interactions of compound A in (a) Auto Dock VINA and (b) CLCDDW.

The molecular interactions of compound A in the active site using Auto Dock Vina includes a π-σ interaction with ALA 221 and ILE 295 and alkyl interactions with LYS 248, VAL 245 and PRO 293 whereas the CLCDDW molecular interactions depict conventional hydrogen bonding with GLN 241 and GLN 244, π-cation interaction with LYS 248, π-σ interaction with ILE 295, π-amide stacked interaction with CYS 247 and alkyl interactions with PRO 304. Only ILE 295 residue has similar interactions in both Auto Dock Vina and CLCDDW. However, some of the amino residues in the docking are the same as the residues found experimentally though NMR. These residues include GLN 241, LYS 248, LYS 251, ILE 295, and PRO 293 (Brown et al., 2014).

3.5 Molecular dynamics

MD simulation study for 50 ns time span was performed on complexes of selected hit compounds with the Zaire Ebola virus protein. To verify the dynamic stability between ligand and protein complexes, the RMSD, RMSF and Rg from the MD trajectories were analyzed. The RMSD values of protein backbone were calculated and plotted (Fig. 10). It is observed that all systems are equilibrated during the simulation over 50 ns time span. The trend of trajectories of all

complexes reveals that initially all systems show a little bit of fluctuation up to half of the total simulation time but afterward they become equilibrated. The average RMSD values of entire trajectories give an idea about the fluctuation of the backbone of the system during the MD simulation. The mean values of RMSD are 1.512, 1.304, 1.428, 1.599 and 1.774 nm for the protein-ligand complexes for the selected compounds A, B, C, D and E respectively.

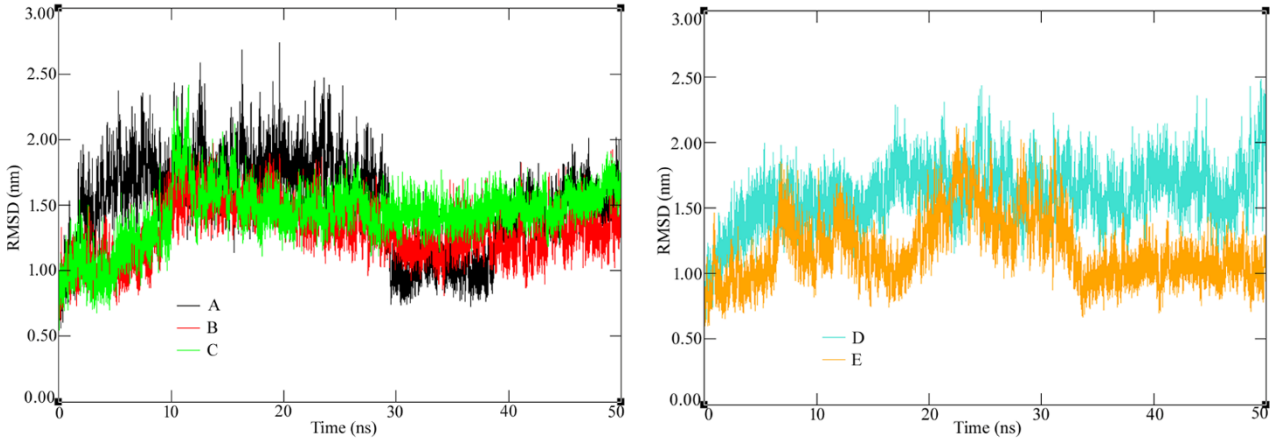

Fig. 10: RMSD versus time of protein-ligand complexes.

Individual amino residues play important roles in the stability of the protein-ligand complex. So, the participation of each amino acid residue in protein-ligand constancy was analyzed by calculation of RMSF values (Fig. 11). RMSF trajectories show that fluctuations of amino residues are found to be higher in around the amino residues 50 to 60, 75 to 90 and 115 to 120. The probable reason of deviation of these amino acids may be a region of the flexible loop and lack of interactions with corresponding ligands. Maximum, minimum and average RMSF values are 3.071, 0.505 and 1.031; 2.272, 0.434 and 0.827; 3.045, 0.504 and 0.876 nm; 2.033, 0.456 and 0.795 nm; and, 1.864, 0.474 and 0.828 nm respectively for the protein-ligand complexes formed from the selected compounds A, B, C, D and E respectively.

The Rg was calculated to explore the firmness of protein-ligand complex systems (Fig. 12). The trajectories undoubtedly explain that all the systems are equilibrated throughout the MD simulation. To analyze the variation of Rg difference between maximum and minimum values were calculated and found to be 1.134, 0.730, 0.898, 0.821 and 0.727 nm for the complex with

molecules A, B, C, D and E respectively. Therefore, detailed analysis of MD simulation study unquestionably shows that all molecules are well equilibrated throughout the simulation.

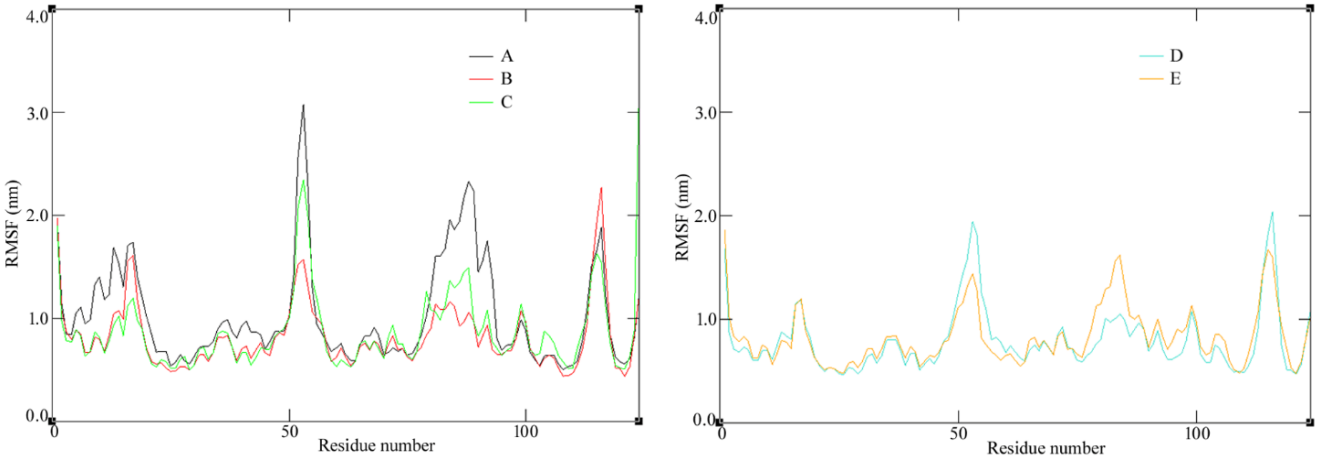

Fig. 11: RMSF versus number of residues of complexes in final proposed molecules.

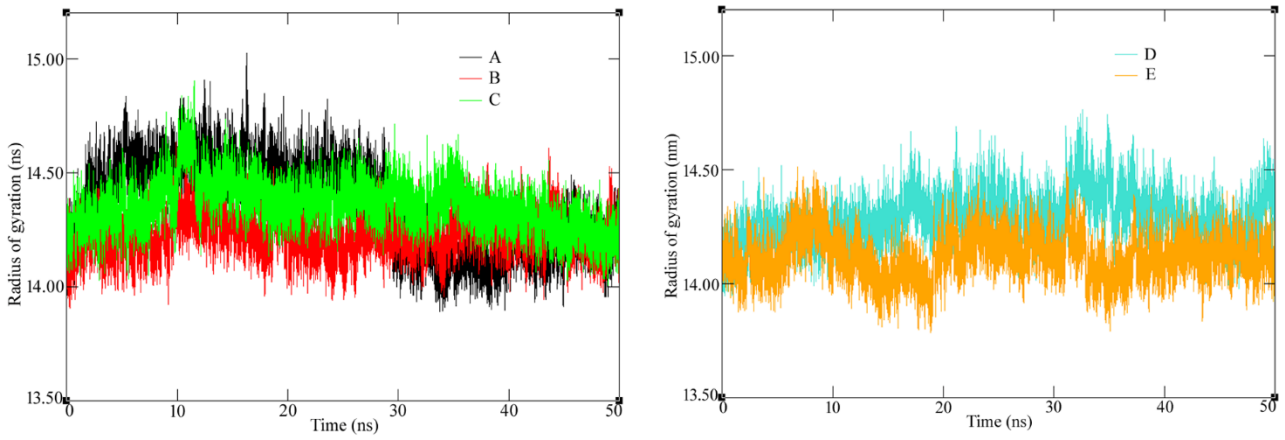

Fig. 12: Radius of gyration versus simulation time.

3.6 Binding energy using MM-GBSA approach

To further check the binding affinity towards the receptor cavity in the simulation study, all protein-ligand complex systems were used to calculate the binding free energy for 50 ns trajectories using the MM-GBSA approach in AMBER14. The total binding free energy (ΔG_{bind}), van der Waals interactions energy (ΔG_{vdW}), electrostatics energy (ΔG_{ele}) and polar solvation energy ($\Delta G_{ele,\ sol}$) (Table 4). The $\Delta \boldsymbol{G_{bind}}$ values using MM-GBSA approach is the contribution of

ΔG_{vdW}, ΔG_{ele} and $\Delta G_{ele,\,sol}$ and are all highly negative for all five compounds (A, B, C, D and E) to further imply strong binding affinity towards the receptor cavity of the Ebola virus protein. However, it was observed that ΔG_{vdW} mainly contributes to the $\Delta \boldsymbol{G_{bind}}$ of the protein-ligand complexes. The strong binding affinities from MM-GBSA method successfully correlates with consensus scores derived using VINA and CLCDDW docking programs.

Table 4: Binding free energies of selected compounds using MM-GBSA approach

Complex	$\Delta \boldsymbol{G_{vdW}}$	$\Delta \boldsymbol{G_{ele}}$	$\Delta \boldsymbol{G_{ele,sol}}$	$\Delta \boldsymbol{G_{bind}}$
A	-38.793	-4.261	8.444	-34.611
B	-39.299	0.532	6.885	-31.883
C	-37.229	-4.882	10.642	-31.469
D	-40.636	-6.067	10.636	-36.067
E	-38.778	-8.472	15.316	-31.935

3.7. Future perspectives

Albeit the in silico prediction often serves as resource-saving approach towards identification of lead compounds, integrating the prediction with experimental high-throughput validation would enable more effective assessments of structure, function and modulation of crucial therapeutic targets, and as such might accelerate the drug discovery process (Bajorath, 2002; Zheng et al., 2018). An efficient and reliable method such as thermal shift assay methodology could be used to assess the predicted hit compounds from our computational studies (Srinivasan, Zhou, Kubanek, & Skolnick, 2014). These hit compounds could be experimentally assessed for binding by thermal-melt assays, followed by their physiological functions against the EBOV. By extension, experimental studies that involve kinetic studies of binding and unbinding events or the drug-protein residence time could also offer a good experiment-based understanding of inhibitory effect of a drug being developed (Prada-Gracia, Huerta-Yépez, & Moreno-Vargas, 2016).

4. Conclusion

Reoccurrence of Ebola outbreaks and none availability of a licensed drug for the treatment of EVD necessitate continuous research efforts towards designing and making drugs that can effectively curb the menace of EBOV. Consensus scoring approach to virtual screening of significantly large database of about 36 million molecules against the crystal structure of notorious Zaire Ebola viral protein 35 led to the selection of five compounds with potentials of becoming antiviral drugs for EVD. The binding energy values were found to be -8.4, -7.9, -8.0, -8.1 and to -8.9 kcal/mol for compound A, B, C, D, and E respectively, and their physiological and bioactivity properties, as well as ADMET properties were predicted to be good. Compound A appeared to be the most promising of the five selected compounds with respect to its bioavailability radar and K_i value (0.7 µM). The 50-ns molecular dynamics simulation results gave RMSD, RMSF and Rg values which showed that all proposed molecules were well equilibrated and hence stable in the protein-ligand complexes. The observed strong binding affinities of the selected compounds with the receptor cavity agreed with the docking analysis results. It is speculated that the use of consensus scoring method enhanced the agreement between the docking analysis and MD simulations. Furthermore, the observed molecular interactions in both employed docking protocols, Auto Dock Vina and CLCDDW, were the same as those discovered experimentally. The need to experimentally validate the *in silico* results reported herein with non-trivial *in vitro* and/or *in vivo* inhibition measurements is acknowledged but lack of funding limited this work. It is thus envisioned these identified inhibitors will serve as a better starting point for further experimental studies in the antiviral drug discovery process.

Conflict of interest

The authors declare no conflict of interest and we all approved this article for publication.

Acknowledgments

MA Islam would like to appreciate National Research Foundation (NRF), South Africa for Innovation Post-Doctoral Fellowship. MA Islam is thankful to the CHPC (www.chpc.ac.za) for providing computational resources.

Printed version of figures

Black and white in print is required.

References

Andersen, H. C. (1983). Rattle: A “velocity” version of the shake algorithm for molecular dynamics calculations. *Journal of Computational Physics*, *52*(1), 24–34. http://doi.org/10.1016/0021-9991(83)90014-1

Bah, E. I., Lamah, M.-C., Fletcher, T., Jacob, S. T., Brett-Major, D. M., Sall, A. A., Fowler, R. A. (2015). Clinical Presentation of Patients with Ebola Virus Disease in Conakry, Guinea. *New England Journal of Medicine*, *372*(1), 40–47. http://doi.org/10.1056/NEJMoa1411249

Bajorath, J. (2002). Integration of virtual and high-throughput screening. *Nat Rev Drug Discov.*, *1*(11), 882–894. http://doi.org/10.1038/nrd941

Barcellos, M. P., Santos, C. B. R., Federico, L. B., Almeida, P. F., da Silva, C., & Taft, C. A. (2018). Pharmacophore and structure-based drug design, molecular dynamics and admet/tox studies to design novel potential pad4 inhibitors. *Journal of Biomolecular Structure and Dynamics*, (12), 1–16. http://doi.org/10.1080/07391102.2018.1444511

BIOVIA, D. S. (2015). Discovery Studio Modeling Environment. San Diego: Dassault Systèmes.

Brown, C. S., Lee, M. S., Leung, D. W., Wang, T., Xu, W., Luthra, P., Amarasinghe, G. K. (2014). In silico derived small molecules bind the filovirus VP35 protein and inhibit its polymerase cofactor activity. *Journal of Molecular Biology*, *426*(10), 2045–2058. http://doi.org/10.1016/j.jmb.2014.01.010

Bukreyev, A. A., Chandran, K., Dolnik, O., Dye, J. M., Ebihara, H., Leroy, E. M., Kuhn, J. H. (2014). Discussions and decisions of the 2012–2014 International Committee on Taxonomy of Viruses (ICTV) Filoviridae Study Group, January 2012–June 2013. *Archives of Virology*, *159*(4), 821–830. http://doi.org/10.1007/s00705-013-1846-9

Camp, D., Garavelas, A., & Campitelli, M. (2015). Analysis of Physicochemical Properties for Drugs of Natural Origin. http://doi.org/10.1021/acs.jnatprod.5b00255

Cavuturu, B. M., Bhandare, V. V., Ramaswamy, A., & Arumugam, N. (2018). Molecular dynamics of interaction of Sesamin and related compounds with the cancer marker β-catenin: an *in silico* study. *Journal of Biomolecular Structure and Dynamics*, 1–15. http://doi.org/10.1080/07391102.2018.1442250

Cerqueira, N. M. F. S. A., Gesto, D., Oliveira, E. F., Santos-Martins, D., Brás, N., Sousa, S. F.,

… Ramos, M. J. (2015). Receptor-based virtual screening protocol for drug discovery. *Archives of Biochemistry and Biophysics*, *582*, 56–67. http://doi.org/10.1016/j.abb.2015.05.011

Choi, J. H., Jonsson-Schmunk, K., Qiu, X., Shedlock, D. J., Strong, J., Xu, J. X., Croyle, M. A. (2015). A Single Dose Respiratory Recombinant Adenovirus-Based Vaccine Provides Long-Term Protection for Non-Human Primates from Lethal Ebola Infection. *Molecular Pharmaceutics*, *12*(8), 2712–2731. http://doi.org/10.1021/mp500646d

Daina, A., Michielin, O., & Zoete, V. (2017). SwissADME : a free web tool to evaluate pharmacokinetics , drug- likeness and medicinal chemistry friendliness of small molecules. *Nature Publishing Group*, (October 2016), 1–13. http://doi.org/10.1038/srep42717

Delgado-Soler, L., Ariñez-Soriano, J., Granadino-Roldán, J. M., & Rubio-Martinez, J. (2011). Predicting binding energies of CDK6 inhibitors in the hit-to-lead process. *Theoretical Chemistry Accounts*, *128*(4–6), 807–823. http://doi.org/10.1007/s00214-010-0857-9

Feher, M. (2006). Consensus scoring for protein-ligand interactions. *Drug Discovery Today*, *11*(9–10), 421–428. http://doi.org/10.1016/j.drudis.2006.03.009

Feldmann, H., Geisbert, T. W., Leung, A., al., et, Collins, P., Bukreyev, A., & Hensley, L. (2011). Ebola haemorrhagic fever. *The Lancet*, *377*(9768), 849–862. http://doi.org/10.1016/S0140-6736(10)60667-8

Genheden, S., & Ryde, U. (2015). Expert Opinion on Drug Discovery The MM / PBSA and MM / GBSA methods to estimate ligand-binding affinities The MM / PBSA and MM / GBSA methods to estimate ligand-binding affinities. *Expert Opinion on Drug Discovery*, *10*(5), 0. http://doi.org/10.1517/17460441.2015.1032936

Grard, G., Biek, R., Muyembe Tamfum, J.-J., Fair, J., Wolfe, N., Formenty, P., Leroy, E. (2011). Emergence of Divergent Zaire Ebola Virus Strains in Democratic Republic of the Congo in 2007 and 2008. *Journal of Infectious Diseases*, *204*(suppl 3), S776–S784. http://doi.org/10.1093/infdis/jir364

Haasnoot, J., de Vries, W., Geutjes, E.-J., Prins, M., de Haan, P., & Berkhout, B. (2007). The Ebola Virus VP35 Protein Is a Suppressor of RNA Silencing. *PLoS Pathogens*, *3*(6), e86. http://doi.org/10.1371/journal.ppat.0030086

Hajduk, P. J., Huth, J. R., & Tse, C. (2005). Predicting protein druggability. *Drug Discovery Today*, *10*(23–24), 1675–1682. http://doi.org/10.1016/S1359-6446(05)03624-X

Hooft, R. W., Sander, C., & Vriend, G. (1997). Objectively judging the quality of a protein structure from a Ramachandran plot. *Computer Applications in the Biosciences : CABIOS*, *13*(4), 425–430. http://doi.org/10.1093/bioinformatics/13.4.425

Hopkins, A. L., Groom, C. R., & Alex, A. (2004). Ligand efficiency: A useful metric for lead selection. *Drug Discovery Today*, *9*(10), 430–431. http://doi.org/10.1016/S1359-6446(04)03069-7

Hughes, J., Rees, S., Kalindjian, S., & Philpott, K. (2011). Principles of early drug discovery. *British Journal of Pharmacology*, *162*(6), 1239–1249. http://doi.org/10.1111/j.1476-5381.2010.01127.x

Islam, M. A., & Pillay, T. S. (2018). β-secretase inhibitors for Alzheimer's disease: identification using pharmacoinformatics. *Journal of Biomolecular Structure and Dynamics*, 1–20. http://doi.org/10.1080/07391102.2018.1430619

Jedrzejas, M. J., Singh, S., Brouillette, W. J., Air, G. M., & Luo, M. (1995). A strategy for theoretical binding constant, Ki, calculations for neuraminidase aromatic inhibitors designed on the basis of the active site structure of influenza virus neuraminidase. *Proteins: Structure, Function, and Bioinformatics*, *23*(2), 264–277. http://doi.org/10.1002/prot.340230215

Kapetanovic, I. M. (2008). Computer-aided drug discovery and development (CADDD): In silico-chemico-biological approach. *Chemico-Biological Interactions*, *171*(2), 165–176. http://doi.org/10.1016/j.cbi.2006.12.006

Kiss, R., Sandor, M., & Szalai, F. a. (2012). http://Mcule.com: a public web service for drug discovery. *Journal of Cheminformatics*, *4*(Suppl 1), P17. http://doi.org/10.1186/1758-2946-4-S1-P17

Kleywegt, G. J., & Jones, T. A. (1996). Phi/Psi-chology: Ramachandran revisited. *Structure*, *4*(12), 1395–1400. http://doi.org/10.1016/S0969-2126(96)00147-5

Knudsen, Bjarne Knudsen, T. (2016). CLC Drug Discovery Workbench. Retrieved from http://www.clcsupport.com/clcdrugdiscoveryworkbench/current/User_Manual.pdf

Kuhn, J. H., Becker, S., Ebihara, H., Geisbert, T. W., Johnson, K. M., Kawaoka, Y., Jahrling, P. B. (2010). Proposal for a revised taxonomy of the family Filoviridae: classification, names of taxa and viruses, and virus abbreviations. *Archives of Virology*, *155*(12), 2083–2103. http://doi.org/10.1007/s00705-010-0814-x

Leung, D. W., Shabman, R. S., Farahbakhsh, M., Prins, K. C., Borek, D. M., Wang, T., Amarasinghe, G. K. (2010). Structural and Functional Characterization of Reston Ebola Virus VP35 Interferon Inhibitory Domain. *Journal of Molecular Biology*, *399*(3), 347–357. http://doi.org/10.1016/j.jmb.2010.04.022

Lindorff-Larsen, K., Piana, S., Palmo, K., Maragakis, P., Klepeis, J. L., Dror, R. O., & Shaw, D. E. (2010). Improved side-chain torsion potentials for the Amber ff99SB protein force field. *Proteins: Structure, Function, and Bioinformatics*, NA-NA. http://doi.org/10.1002/prot.22711

Lipinski, C. A. (2000). Drug-like properties and the causes of poor solubility and poor permeability. *Journal of Pharmacological and Toxicological Methods*, *44*(1), 235–249. http://doi.org/10.1016/S1056-8719(00)00107-6

Lipinski, C. A. (2004). Lead- and drug-like compounds: The rule-of-five revolution. *Drug Discovery Today: Technologies*, *1*(4), 337–341. http://doi.org/10.1016/j.ddtec.2004.11.007

Lipinski, C. A., Lombardo, F., Dominy, B. W., & Feeney, P. J. (2001). Experimental and computational approaches to estimate solubility and permeability in drug discovery and development settings. *Advanced Drug Deliv. Rev.*, *46*(1–3), 3–26. http://doi.org/10.1016/S0169-409X(96)00423-1

Lovell, S. C., Davis, I. W., Arendall, W. B., de Bakker, P. I. W., Word, J. M., Prisant, M. G., Richardson, D. C. (2003). Structure validation by Cα geometry: ϕ,ψ and Cβ deviation. *Proteins: Structure, Function, and Bioinformatics*, *50*(3), 437–450. http://doi.org/10.1002/prot.10286

Mirza, M. U., & Ikram, N. (2016). Integrated computational approach for virtual hit identification against ebola viral proteins VP35 and VP40. *International Journal of Molecular Sciences*, *17*(11). http://doi.org/10.3390/ijms17111748

Olsson, M. H. M., Søndergaard, C. R., Rostkowski, M., & Jensen, J. H. (2011). PROPKA3: Consistent Treatment of Internal and Surface Residues in Empirical pKa Predictions. *Journal of Chemical Theory and Computation*, *7*(2), 525–37. http://doi.org/10.1021/ct100578z

Onawole, A. T., Kolapo, T. U., Sulaiman, K. O., & Adegoke, R. O. (2018). Structure based virtual screening of the Ebola virus trimeric glycoprotein using consensus scoring. *Computational Biology and Chemistry*, *72*, 170–180.

http://doi.org/10.1016/j.compbiolchem.2017.11.006

Onawole, A. T., Sulaiman, K. O., Adegoke, R. O., & Kolapo, T. U. (2017). Identification of potential inhibitors against the Zika virus using consensus scoring. *Journal of Molecular Graphics and Modelling*, *73*, 54–61. http://doi.org/10.1016/j.jmgm.2017.01.018

Pecina, A., Haldar, S., Fanfrlik, J., Meier, R., Řezáč, J., Lepsik, M., & Hobza, P. (2017). The SQM/COSMO Scoring Function at the DFTB3-D3H4 Level: Unique Identification of Native Protein-Ligand Poses. *Journal of Chemical Information and Modeling*, *57*, 127–132. http://doi.org/10.1021/acs.jcim.6b00513

Pires, D. E. V., Blundell, T. L., & Ascher, D. B. (2015). pkCSM: Predicting small-molecule pharmacokinetic and toxicity properties using graph-based signatures. *Journal of Medicinal Chemistry*, *58*(9), 4066–4072. http://doi.org/10.1021/acs.jmedchem.5b00104

Polanski, J., Tkocz, A., & Kucia, U. (2017). Beware of ligand efficiency (LE): understanding LE data in modeling structure ‐ activity and structure ‐ economy relationships. *Journal of Cheminformatics*, *9*(49), 1–8. http://doi.org/10.1186/s13321-017-0236-9

Prada-Gracia, D., Huerta-Yépez, S., & Moreno-Vargas, L. M. (2016). Application of computational methods for anticancer drug discovery, design, and optimization. *Boletín Médico Del Hospital Infantil de México*, *73*(6), 411–423. http://doi.org/10.1016/j.bmhimx.2016.10.006

Radchenko, E. V., Dyabina, A. S., Palyulin, V. A., & Zefirov, N. S. (2016). Prediction of human intestinal absorption of drug compounds from molecular structure. *Russian Chemical Bulletin*, *65*(2), 576–580. http://doi.org/10.1021/CI980029A

Ramachandran, G. N., & Sasisekharan, V. (1968). Conformation of Polypeptides and Proteins. *Advances in Protein Chemistry*, *23*, 283–437. http://doi.org/10.1016/S0065-3233(08)60402-7

Ren, J.-X., Zhang, R.-T., Zhang, H., Cao, X.-S., Liu, L.-K., & Xie, Y. (2016). Identification of novel VP35 inhibitors: Virtual screening driven new scaffolds. *Biomedicine & Pharmacotherapy*, *84*, 199–207. http://doi.org/10.1016/J.BIOPHA.2016.09.034

Reynolds, C. H., & Reynolds, R. C. (2017). Group Additivity in Ligand Binding Affinity: An Alternative Approach to Ligand Efficiency. *Journal of Chemical Information and Modeling*, *57*, 3086–3096. http://doi.org/10.1021/acs.jcim.7b00381

Roe, D. R., & Cheatham, T. E. (2013). PTRAJ and CPPTRAJ: Software for Processing and

Analysis of Molecular Dynamics Trajectory Data. *Journal of Chemical Theory and Computation*, *9*(7), 3084–3095. http://doi.org/10.1021/ct400341p

Salomon-Ferrer, R., Case, D. A., & Walker, R. C. (2013). An overview of the Amber biomolecular simulation package. *Wiley Interdisciplinary Reviews: Computational Molecular Science*, *3*(2), 198–210. http://doi.org/10.1002/wcms.1121

Sanguinetti, M. C., & Tristani-firouzi, M. (2006). hERG potassium channels and cardiac arrhythmia, *440*(March), 463–469. http://doi.org/10.1038/nature04710

Schwede, T. (2013). Homology Modeling of Protein Structures. In *Encyclopedia of Biophysics* (pp. 992–998). Berlin, Heidelberg: Springer Berlin Heidelberg. http://doi.org/10.1007/978-3-642-16712-6_417

Setlur, A. S., Naik, S. Y., & Skariyachan, S. (2017). Herbal Lead as Ideal Bioactive Compounds Against Probable Drug Targets of Ebola Virus in Comparison with Known Chemical Analogue: A Computational Drug Discovery Perspective. *Interdisciplinary Sciences: Computational Life Sciences*, *9*(2), 254–277. http://doi.org/10.1007/s12539-016-0149-8

Srinivasan, B., Zhou, H., Kubanek, J., & Skolnick, J. (2014). Experimental validation of FINDSITE comb virtual ligand screening results for eight proteins yields novel nanomolar and micromolar binders. *Joiurnal of Cheminformatics*, *6*(16), 1–14.

The World Bank. (2015, August). GDP growth (annual %). http://doi.org/10.1016/S2214-109X(15)00065-0

Toropov, A. A., Toropova, A. P., Beeg, M., Gobbi, M., & Salmona, M. (2017). QSAR model for blood-brain barrier permeation. *Journal of Pharmacological and Toxicological Methods*, *88*, 7–18. http://doi.org/10.1016/j.vascn.2017.04.014

Tosh, P. K., Sampathkumar, P., Feldmann, H., & al., et. (2014). What clinicians should know about the 2014 Ebola outbreak. *Mayo Clinic Proceedings*, *89*(12), 1710–7. http://doi.org/10.1016/j.mayocp.2014.10.010

Trott, O., & Olson, A. (2010). AutoDock Vina: improving the speed and accuracy of docking with a new scoring function, efficient optimization and multithreading. *Journal of Computational Chemistry*, *31*(2), 455–461. http://doi.org/10.1002/jcc.21334.AutoDock

Tsaioun, K., & Kates, S. (2011). *ADMET for Medicinal Chemists: A Practical Guide*. New Jersey: Wiley.

Villaseñor-Granados, T., García, S., Vazquez, M. A., & Robles, J. (2016). Molecular docking-

based screening of newly designed coumarin derivatives with potential antifungal activity against lanosterol 14 α-demethylase. *Theoretical Chemistry Accounts*, *135*(9), 210. http://doi.org/10.1007/s00214-016-1965-y

Wang, J., Wang, W., Kollman, P. A., & Case, D. A. (2006). Automatic atom type and bond type perception in molecular mechanical calculations. *Journal of Molecular Graphics and Modelling*, *25*(2), 247–260. http://doi.org/10.1016/J.JMGM.2005.12.005

Wang, J., Wolf, R. M., Caldwell, J. W., Kollman, P. A., & Case, D. A. (2004). Development and testing of a general amber force field. *Journal of Computational Chemistry*, *25*(9), 1157–1174. http://doi.org/10.1002/jcc.20035

Wang, Z., Sun, H., Yao, X., Li, D., Xu, L., Li, Y., … Hou, T. (2016). Comprehensive evaluation of ten docking programs on a diverse set of protein–ligand complexes: the prediction accuracy of sampling power and scoring power. *Phys. Chem. Chem. Phys.*, *18*(18), 12964–12975. http://doi.org/10.1039/C6CP01555G

Wessel, M. D., Jurs, P. C., Tolan, J. W., & Muskal, S. M. (1998). Prediction of human intestinal absorption of drug compounds from molecular structure. *Journal of Chemical Information and Computer Sciences*, *38*(4), 726–35. Retrieved from http://www.ncbi.nlm.nih.gov/pubmed/9691477

Weyer, J., Grobbelaar, A., & Blumberg, L. (2015). Ebola Virus Disease: History, Epidemiology and Outbreaks. *Current Infectious Disease Reports*, *17*(5), 21. http://doi.org/10.1007/s11908-015-0480-y

WHO. (1978). Ebola haemorrhagic fever in Zaire , 1976. *Bulletin of the World Health Organisation*, *56*(October 1976), 271–293.

WHO | WHO Director-General briefs media on outcome of Ebola Emergency Committee. (2016). *WHO*. Retrieved from http://www.who.int/mediacentre/news/statements/2016/ihr-emergency-committee-ebola/en/

Wildman, S. A., & Crippen, G. M. (1999). Prediction of Physicochemical Parameters by Atomic Contributions. http://doi.org/10.1021/CI990307L

Xu, W., Lucke, A. J., & Fairlie, D. P. (2015). Comparing sixteen scoring functions for predicting biological activities of ligands for protein targets. *Journal of Molecular Graphics and Modelling*, *57*, 76–88. http://doi.org/10.1016/j.jmgm.2015.01.009

Ye, L., & Yang, C. (2015). Development of vaccines for prevention of Ebola virus infection.

Microbes and Infection, *17*(2), 98–108. http://doi.org/10.1016/j.micinf.2014.12.004

Zheng, M., Li, X., Li, F., Luo, X., Zhao, J., Cui, C., Chen, K. (2018). Computational chemical biology and drug design : Facilitating protein structure , function , and modulation studies. *Medicinal Research Reviews*, *38*(3), 914–950. http://doi.org/10.1002/med.21483